

# Heat Transfer Characteristics of Acoustic Streaming by Longitudinal Ultrasonic Vibration

Byoung-Gook Loh\*

*Hansung University, Seoul 136-792, Republic of Korea*

and

Dong-Ryul Lee†

*Catholic University of Daegu, Kyungbuk 712-702, Republic of Korea*

Heat transfer characteristics of acoustic streaming generated by longitudinal ultrasonic vibration at 30 kHz are presented. To investigate the enhancement of heat transfer capability of acoustic streaming, the temperature variations of the heat source and air in the vicinity of the heat source are measured in real time. It is observed that ultrasonic vibration instantly induces acoustic streaming and results in the significant temperature drop as a result of the bulk airflow caused by acoustic streaming. The cooling effect on the heat source is found to have strong correlation with the gap between the ultrasonic vibrator and heat source; the cooling effect is maximized when the gap corresponds to the multiple of half-wavelength of the ultrasonic wave. This result is attributable to the resonance of the sound wave. The theoretical analysis of the dependence of cooling capability of acoustic streaming on the gap is performed as well. Temperature distribution in the gap along the radius and the direction normal to the vibrating surface is measured while acoustic streaming is induced. Variations of temperature drop along the radius are not observed, but temperature drop significantly decreases with the distance from the heat source. The advantage of the cooling method using acoustic streaming is noise free because of the ultrasonic vibration. Moreover, this cooling method can be applied to the micro-electro-mechanical systems, where the fan-based conventional cooling method cannot be employed.

## Nomenclature

$F$	= nonlinear driving forcing term, N
$H$	= gap between the vibrating surface and stationary surface, m
$h$	= heat transfer coefficient of the fluid, W/m <sup>2</sup> K
$i$	= imaginary operator
$K$	= acoustic wave number ( $2\pi/\lambda$ ), rad/m
$k$	= thermal conductivity of the fluid, W/mK
$L$	= characteristic length, m
$Nu$	= local Nusselt number, $hL/k$
$P_2$	= steady-state dc pressure, Pa
$R$	= radius of the heat source, m
$r$	= coordinate in radial direction, m
$t$	= time, s
$U_L$	= time-independent limiting velocity, m/s
$U_0$	= amplitude of irrotational velocity tangent to the boundary, m/s
$u_1$	= oscillatory particle velocity, m/s
$u_2$	= acoustic streaming velocity, m/s
$V$	= normal irrotational velocity, m/s
$X$	= coordinate tangent to the boundary, m
$z$	= coordinate normal to the vibrating surface, m
$\lambda$	= wavelength, m
$\mu$	= dynamic viscosity of the fluid, Pa · s
$\xi$	= air particle displacement, m
$\xi_0$	= peak vibration amplitude, m
$\rho_0$	= constant equilibrium density, m <sup>3</sup> /kg
$\omega$	= excitation frequency, rad/s

## Introduction

ACOUSTIC streaming is a vortex-type airflow caused by a high-intensity sound wave. Two factors have been known to induce acoustic streaming: spatial attenuation of a wave in free space and the friction between a medium and a vibrating object.<sup>1–3</sup> The absorption and scattering of the sound wave result in the attenuation of the sound wave in the process of the propagation. This attenuation is in general considered negligible, but the propagation of a high-intensity sound wave causes the attenuation of pressure significant enough to create a steady bulk airflow.<sup>4,5</sup> This type of streaming usually occurs in a medium of high viscosity. The other type of acoustic streaming is attributable to the friction between a medium and a solid wall when the former is vibrating in contact with the latter or vice versa.<sup>6</sup> This study focuses on this kind of near boundary acoustic streaming. The acoustic streaming is especially effective in promoting certain kinds of rate process occurring on the solid and fluid interface including convective heat transfer, electrical effects, changes in biological cells, and removal of loosely adhering surface layers.<sup>6</sup>

Faraday first observed the phenomenon of acoustic streaming.<sup>7</sup> The theoretical analysis of acoustic streaming was performed by Rayleigh,<sup>8</sup> Schlichting,<sup>9</sup> Nyborg,<sup>6</sup> and Lighthill.<sup>4</sup> Gopinath and Mills investigated convective heat transfer caused by acoustic streaming across the ends of a Kundt tube.<sup>10,11</sup> Vainshtein et al.<sup>12</sup> and Uhlenwinkel et al.<sup>13</sup> investigated the heat transfer characteristics of acoustic streaming. Wan and Kuznetsov numerically modeled the effect of acoustic streaming.<sup>14–16</sup> Loh et al.<sup>2</sup> and Ro et al.<sup>3</sup> studied the enhancement of heat transfer by acoustic streaming induced by ultrasonic flexural vibration.

Among the previous studies, Loh and Ro's study is notable in that it is the first experiment performed in an open channel and that the significant amount of temperature drop is achieved. The nature of heat transfer characteristics of acoustic streaming in an open channel is three-dimensional. The complexity of the acoustic streaming by ultrasonic vibration allows for only minimal analysis of the problem with analytical method. Three-dimensional computational-fluid-dynamics (CFD) analysis is the only method available to fully understand the acoustic streaming phenomenon but is not an easy task because of the long computational hours required

Received 25 February 2003; revision received 5 August 2003; accepted for publication 6 August 2003. Copyright © 2003 by the American Institute of Aeronautics and Astronautics, Inc. All rights reserved. Copies of this paper may be made for personal or internal use, on condition that the copier pay the \$10.00 per-copy fee to the Copyright Clearance Center, Inc., 222 Rosewood Drive, Danvers, MA 01923; include the code 0887-8722/04 \$10.00 in correspondence with the CCC.

\*Professor, Department of Mechanical Systems Engineering.

†Professor, School of Mechanical and Automotive Engineering, 330 Keum Rak 1-ri, Hayang-Eup, Kyungsan; dlee@cu.ac.kr.

for the analysis resulting from the high excitation frequency and the moving-wall-boundary condition. Without three-dimensional analysis in-depth understanding of the heat transfer characteristics of acoustic streaming might not be obtained.

The objective of this study is to construct experimental apparatus enabling three-dimensional heat transfer analysis of acoustic streaming and to collect experimental data that serve as a preliminary three-dimensional experimental investigation of acoustic streaming phenomenon validating the three-dimensional CFD analysis to be performed. To this end, the experimental apparatus is constructed axisymmetrically by using cylindrical ultrasonic vibrator and the circular heat source. This reduces the computational time for the analysis significantly. In addition, multiple thermocouples are placed in the neighborhood of the heat source and ultrasonic vibrator to measure the change in the temperature as a result of acoustic streaming, which enables the calculation of the local Nusselt number to characterize the heat transfer enhancement by acoustic streaming.

In addition to the advantage that acoustic streaming is silent cooling, this novel cooling method can be applied to where the conventional motor-driven cooling method cannot be employed such as micro-electro-mechanical system by using thin-film piezoelectric devices.<sup>3</sup> Therefore, it is necessary to fully understand the heat transfer characteristics of acoustic streaming in order to use this promising technology practically.

### Theoretical Background

Following Nyborg's formulation, the equation for near-boundary acoustic streaming can be expressed as

$$\mu \nabla^2 u_2 - \nabla P_2 + F = 0 \quad (1)$$

$$F \equiv -\rho_0 \langle (u_1 \cdot \nabla) u_1 + u_1 (\nabla \cdot u_1) \rangle \quad (2)$$

where  $\langle \rangle$  means a time average over a large number of cycles.<sup>6</sup> Without averaging,  $F$  contains a dc part and harmonically varying terms. When averaged over a long period of time, the effect of harmonically varying forcing terms cancels, and only the contributions from the dc part remain in the solution. This dc part generates acoustic streaming. The acoustic streaming velocity  $u_2$  approaches a constant

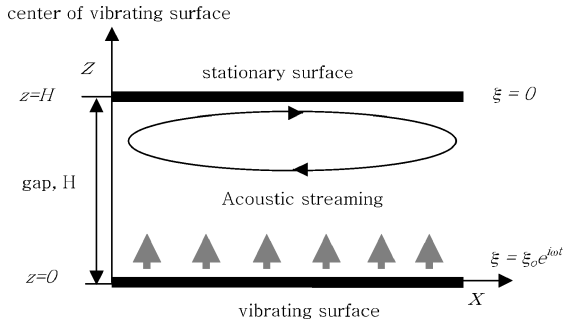


Fig. 1 Simplified schematic diagram of the experimental setup.

value as the distance from the vibrating surface approaches infinity. This time-independent limiting velocity  $U_L$  is given by

$$-\frac{3}{4\omega} U_0 \left( \frac{dU_0}{dx} \right) \quad (3)$$

where  $x$  is the direction tangent to the boundary.<sup>17</sup> To calculate outer acoustic streaming motion, the limiting velocity  $U_L$  is used as a slip velocity at the solid surface by assuming Stoke boundary-layer thickness negligible.<sup>4</sup>

The amplitude of the tangential irrotational velocity  $U_0$  is calculated from the normal irrotational velocity  $V$  imposing the zero-divergence condition. To calculate  $V$  for the case in Fig. 1, it is assumed the vibrating surface is vibrating in harmonic motion as  $\xi(z, t) = \xi(0, t) = \xi_0 e^{i\omega t}$  and the top surface is stationary. In addition, it is assumed that the radius of the vibrating and stationary surface is sufficiently large compared to the wavelength of the ultrasonic wave. Employing linear acoustics theory and imposing the boundary conditions  $\xi = \xi_0 e^{i\omega t}$  at  $z = 0$  and  $\xi = 0$  at  $z = H$ , the air particle displacement is obtained as

$$\xi(z, t) = \xi_0 \frac{\sin K(H - z)}{\sin KH} e^{i\omega t} \quad (4)$$

where  $k$  is acoustic wave number and  $H$  is the gap between the vibrating surface and stationary surface as shown in Fig. 1. Taking the time derivative of Eq. (4),  $V$  can be readily derived. And by making use of the zero-divergence condition  $\partial U_0 / \partial x + \partial V / \partial z = 0$ , the amplitude of the tangential velocity  $U_0$  is given by

$$U_0 = i \xi_0 \omega K \frac{\cos K(H - z)}{\sin KH} x e^{i\omega t} \quad (5)$$

In Eq. (5) it is noted that  $U_0$  is at maximum when  $kH = n\pi$  ( $n = 0, 1, 2, \dots$ ). The purpose of Eq. (5) is not to quantitatively calculate the acoustic streaming velocity but to qualitatively explain a drastic increase in the temperature drop at certain gaps. The effect of a damping term should be considered to calculate the acoustic streaming velocity when  $KH = n\pi$ . But because there exists discontinuity in the boundary conditions, precise quantitative analysis of the acoustic streaming velocity in an analytical way is extremely difficult. For the purpose of explaining a trend of the increased temperature drops at gaps corresponding to  $n\pi/K$ , a simpler equation without the damping term can be employed. Using  $K = 2\pi/\lambda$ , the gap inducing the maximum normal irrotational velocity is derived as  $H = n\lambda/2$ . Therefore, when the gap between the heat source and vibrating surface corresponds to the multiple of half-wavelength of the sound wave, the tangential irrotational velocity  $U_0$  is at maximum, resulting in the maximum acoustic streaming velocity.

### Experimental Setup

The experimental setup shown in Fig. 2 is comprised of bolted-Langevin-type transducer (BLT), horn, heat source, ultrasonic signal generator, and real-time data-acquisition system.<sup>18</sup> The BLT is designed to resonate at 30 kHz. The horn, mechanical vibration

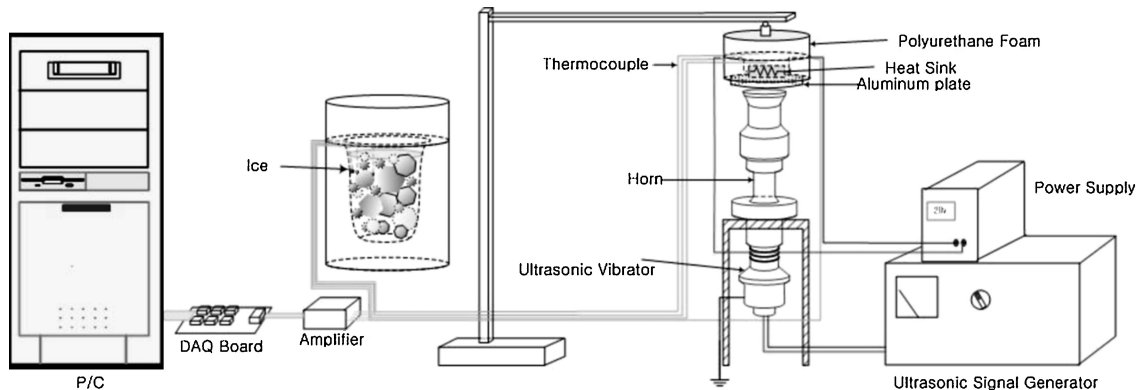


Fig. 2 Schematic diagram of the experimental setup.

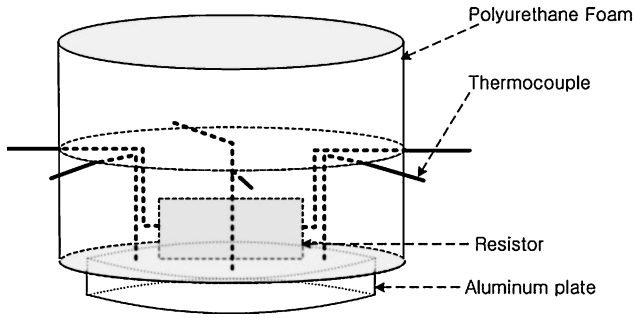


Fig. 3 Detailed schematic of the heat source.

amplifier, designed to resonate at the same frequency as the BLT is attached on the top of the BLT to maximize the vibration amplitude of the system. Mechanical loading of the horn renders the resonance frequency of the BLT shifted within 1 kHz. The resonance frequency shift is compensated by maintaining the impedance of the BLT at minimum because the impedance is minimal at resonance.

The detailed schematic drawing of the heat source is shown in Fig. 3. The heat source consists of resistor, aluminum plate with the same radius of the horn (radius of the horn is 40 mm), thermocouple, and polyurethane foam. Resistor is glued to the aluminum plate using high-temperature-resistance epoxy for heating the aluminum plate. A voltage to the resistor is controlled to heat the heat source to desired temperature. To measure the variation of the temperature of the aluminum plate, four thermocouples are attached to the aluminum plate along a radius of 30 mm with a 90-deg phase difference. The top of the aluminum plate is covered with 40-mm-thick polyurethane foam for insulation, which forces the heat generated by resistor to dissipate only through the one side of the aluminum plate. The electrical signals from thermocouples are amplified and filtered using a low-pass filter before being fed to the data-acquisition board because of the inherent noises of the signal. The vibration amplitude of the BLT is measured with a high-precision capacitance gauge, and the measured amplitude is 50  $\mu\text{m}$ .

## Results and Discussion

### Effect of Ultrasonic Vibration on the Temperature Drop of the Heat Source

To investigate the effect of ultrasonic vibration on the temperature drop, the variations of temperature of the heat source and air in the gap are measured in real time as shown in Fig. 4. Channels (ch) 0–3 represent the temperature variations of four thermocouples attached on the heat source. The variations in the measurements of ch 0–3 are within 5°C because of the difference in the amplification ratio of the respective channel and the voltage vs temperature calibration of thermocouples. To improve the accuracy of the measurements, the measurements of ch 0–3 are averaged, and the averaged measurement is presented in Fig. 4. Ch4 represents the ambient temperature that remains constant throughout the experiment. Ch 5–7 show the temperature variations of air in a gap of 12 mm. Ch5 is located 3 mm above the center of the ultrasonic vibrator. Ch6 is 6 mm, and ch7 is 9 mm above the center of the ultrasonic vibrator. Four watts of power, which is maximum power available for the current experimental setup, is supplied to the resistor in the heat source. The temperature of heat source reaches a steady-state temperature of 163°C in 30 min. Ultrasonic vibration is excited at  $t = 100$  s after the acquisition of the measurements begins with the power to the heat source unchanged and removed at  $t = 500$  s. Temperature of the heat source instantly starts to decrease with ultrasonic vibration and increase as the ultrasonic vibration is removed. A temperature drop of 62°C is achieved in 5 min. Among ch5–7 that represent the temperature variation of air in the gap, ch7 shows the largest temperature prior to ultrasonic vibration excitation because it is located closest to the heat source. The temperatures measured by ch7 drastically diminish at the excitation of the ultrasonic vibration and remain within a band of 10°C fluctuations. Distribution of the acoustic streaming velocity is not uniform along the gap, and the temperature

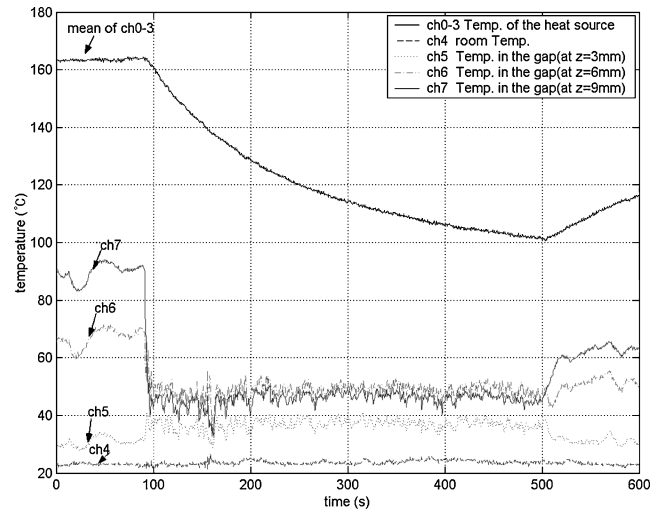


Fig. 4 Temperature vs time without and with ultrasonic vibration.

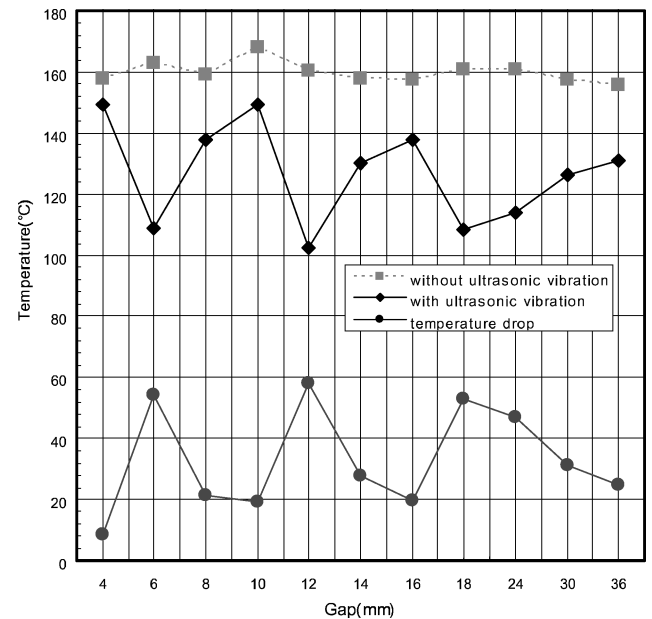


Fig. 5 Temperature vs gap without and with ultrasonic vibration.

drop by acoustic streaming is proportional to the acoustic streaming velocity. It appears that the region in the close vicinity of ch7 has a higher acoustic streaming velocity than the region near ch6 because ch6 has high temperature than ch7, although ch6 is farther from the heat source than ch7. A slight increase in the temperature with ultrasonic vibration is observed for ch5 because of the decline of the intensity of acoustic streaming velocity, and the self-induced heat of ultrasonic vibrator. Near-boundary acoustic streaming stems from the interaction of the radiating sound wave with the physical boundaries. The acoustic streaming velocity decreases as the distance from the physical boundary decreases. Moreover, ultrasonic vibration makes the temperature of the surface of the vibrator grow. As a result, significant heat transfer enhancement is not achieved in the close vicinity of the ultrasonic vibrator.

### Effect of Gap on the Temperature Drop of Heat Source

The dependence of temperature drop on the gap between the ultrasonic vibrator and heat source is investigated. An experiment is performed in accordance with the procedures detailed in the Experimental Setup section, and results are shown in Fig. 5. Square symbols represent the steady-state temperature of the heat source before the ultrasonic vibration is induced. Diamond symbols represent the temperature of the heat source 5 min after the

ultrasonic vibration is excited. Circle symbols show the difference between the temperature with ultrasonic vibration and without ultrasonic vibration. The temperature drop caused by ultrasonic vibration shows strong dependence on the gap and is maximized when the gap coincides with the multiple of 6 mm that is the half-wavelength of the radiating ultrasonic wave. This phenomenon is attributed to the resonance effect of the ultrasonic wave. The detailed theoretical analysis is performed in the Theoretical Background section.

It is well known that conventional fan-based cooling method produces a temperature drop proportional to the distance between the heat source and the fan. However, for cooling using acoustic streaming there exist optimum gaps producing increased heat dissipation as shown in Fig. 5 in which a gap of 6 mm produces temperature drop equivalent to a gap of 12 mm and a gap of 36 mm induces a temperature drop greater than gaps of 8 and 10 mm. It is shown that as the gap increases beyond 18 mm the temperature drop obtained tapers off, although the gap is the multiple of half-wavelength. This is because of a decrease in the intensity of ultrasonic waves caused by propagation loss of the wave. Therefore, it is concluded that the optimum gaps are half-wavelength and one full wavelength, considering the propagation loss.

#### Temperature Distribution in the Gap

To investigate temperature distribution in the gap, temperature along the radius and the gap is measured. With a gap of 24 mm, four thermocouples are located 21 mm above the ultrasonic vibrator. The orientation of four thermocouples is as follows: the first one at  $r =$  the center of the heat source and  $z = 21$  mm, the second one at  $r = R/3$  and  $z = 21$  mm, the third one at  $r = 2R/3$  and  $z = 21$  mm, and the last one at  $r = R$  and  $z = 21$  mm. Temperature variations with and without ultrasonic vibration are measured following the same procedures described in the preceding subsection. Results are shown in Fig. 6. Measurements without ultrasonic vibration marked in square symbols show no variations of temperature along the radius except at  $r = R$ , where the effect of natural convection offsets heat generated by the heat source, resulting in slight increase in temperature compared to ambient temperature ( $22^\circ\text{C}$ ). Temperature instantly drops to  $30^\circ\text{C}$  with ultrasonic vibration excited. The temperature variations along the radius are found to be negligible, which indirectly indicate that airflow induced by acoustic streaming is not confined in the specific region in the gap but considerably uniform along the radius.

To investigate the region affected by acoustic streaming in the gap along the  $z$  direction, the location of four thermocouples is lowered to 21, 18, 15, and 6 mm with the orientation along the  $r$  direction

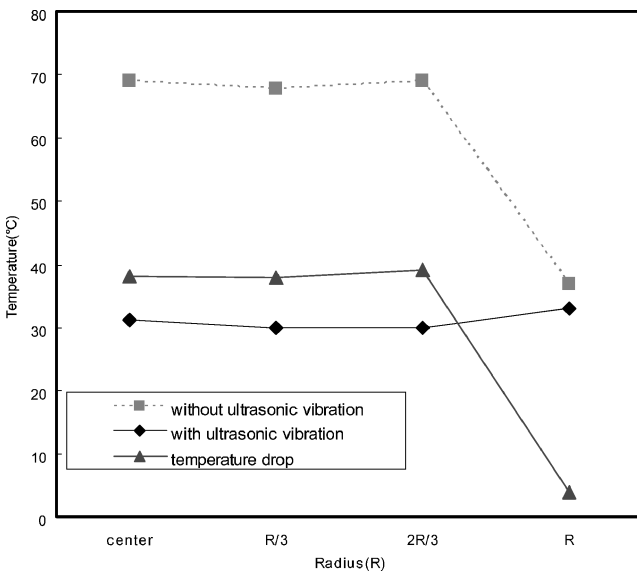


Fig. 6 Temperature vs radius without and with ultrasonic vibration.

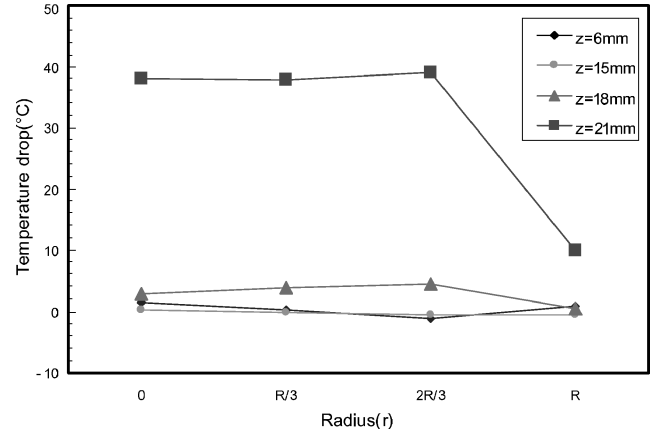


Fig. 7 Temperature drop vs radius with four different  $z$  locations at  $H = 24$  mm.

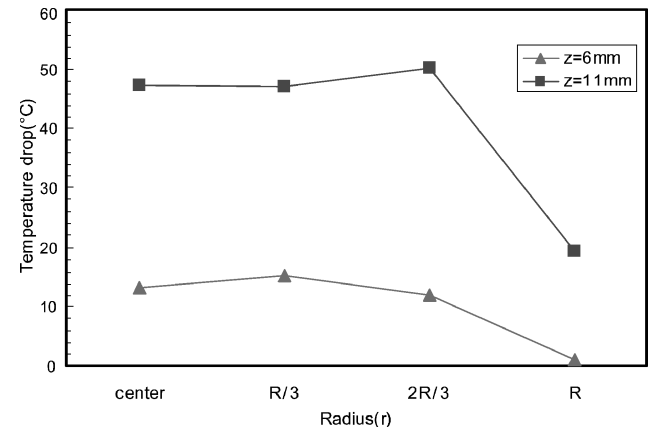


Fig. 8 Temperature drop vs radius with two different  $z$  locations at  $H = 12$  mm.

unchanged. Figure 7 shows a temperature drop produced by acoustic streaming. As the distance from the heat source increases, temperature drop drastically declines, and heat transfer caused by acoustic streaming is not observed when  $z$  is below 18 mm. A similar experiment is performed with a gap of 12 mm and  $z = 3, 6$ , and 11 mm. With  $z$ -coordinate value below 6 mm, cooling by acoustic streaming is not observed. Figure 8 shows a temperature drop with  $z = 6$  and 11 mm.

From this experiment it is concluded that temperature drop along the radius is uniform except the edge of the heat source and that the intensity of acoustic streaming significantly decreases as the distance from the surface of the heat source increases in the  $z$  direction, which is inferred from the drastic decline of the temperature drop. For the experiment with gaps of 12 and 24 mm, the threshold distance, in which significant increase in heat transfer is obtained as a result of acoustic streaming, is found to be 6 mm from the heat source.

#### Effect of the Acoustic Streaming on Heat Transfer

To predict the cooling performance of the proposed system, an extensive study into the nature of heat transfer for the experimental setup shown in Fig. 1 is necessary. The effect of heat transfer enhancement by acoustic streaming between two parallel solid walls kept at different temperatures is analyzed in the preceding section. It is shown that forced airflow increases the rate at which the heat energy dissipates. Because the fluid velocity caused by acoustic streaming is much smaller than that of sound, the flow can be modeled as incompressible. In addition, owing to a relatively small convection velocity, the flow can be regarded as laminar. The buoyance force can be neglected because of the dominance of forced convection.

Mean Nusselt number, which is defined as  $Nu = hL/k$  where  $h$  is heat transfer coefficient by convection measured from the experimental data using Newton's cooling law ( $Q = hA\Delta T$ ) with  $\Delta T (= T_{\text{heat source}} - T_{\text{ambient}})$ ,  $Q_{\text{heat input}}$ ,  $A_{\text{surface area of heat source}}$ ,  $k$  is thermal conductivity of the fluid, and  $L$  is characteristic length of the resonating surface, characterizes the heat transfer enhancement by acoustic streaming. The dependence of Nusselt number on the magnitude of the gap and the local positions ( $r$  and  $z$  direction) in the gap is analyzed.

The effect on heat transfer of the magnitude of the gap between the walls is presented in Fig. 9. It reveals that the variation of Nusselt number caused by the acoustic streaming shows strong dependence on the gap and Nusselt number is found to be a maximum when the gap agrees with the multiple of 6 mm. It is also obvious that there should exist the appropriate gaps for optimum design of the cooling system. Figure 9 also shows a trend similar to the temperature drop as in Fig. 5. A plot of Nusselt number as a function of  $H$  in Fig. 9 indicates a nonlinear relationship that can be fitted well with a power-law correlation.

It is shown that in Figs. 7 and 8 the local temperature drop from the heat source near the stationary surface is significantly higher than that obtained at locations near the oscillating surface. To investigate the effect of the local positions ( $r$  and  $z$ ) on the local heat

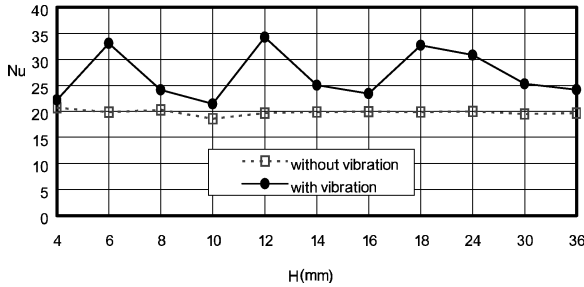


Fig. 9 Nusselt number vs gap ( $H$ ) without and with ultrasonic vibration.

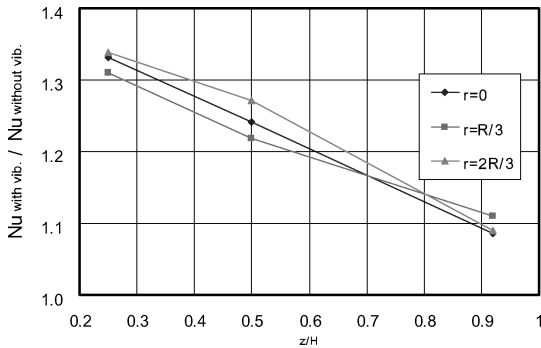


Fig. 10 Nusselt number vs  $z$  locations with three different  $r$  locations at  $H = 12$  mm.

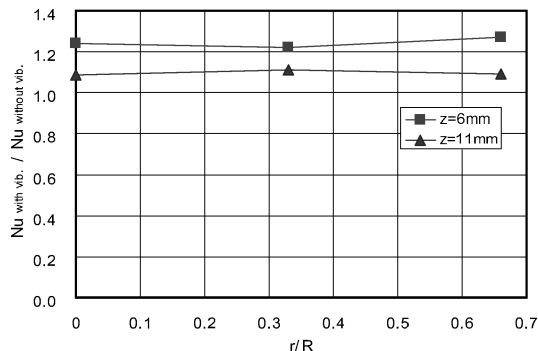


Fig. 11 Nusselt number vs  $r$  locations with two different  $z$  locations at  $H = 12$  mm.

transfer, local Nusselt numbers are calculated for different  $r$  positions ( $r = 0, R/3, 2R/3$ ) and  $z$  positions ( $z = 3, 6, 11$  mm with  $H = 12$  mm). Figure 10 presents the heat transfer results as a function of  $z$  position with respect to the three different  $r$  positions. Relative Nusselt number, which is defined as the ratio of Nusselt number with vibration to that without vibration, gradually decreases with increase in  $z$  position. It is evident that the variation of the positions in the separation gap has a distinct influence on the local Nusselt number. Also, with increases in  $r$  position the heat transfer rate remains unchanged as shown in Fig. 11.

## Conclusions

Real-time measurements of temperature offer an opportunity to better grasp the nature of acoustic streaming in the gap. Exponential decay of temperature in the heat source is observed at the excitation of ultrasonic vibration. Also, strong convective airflow induced by acoustic streaming causes a stepwise temperature drop of air in the close proximity of the heat source. With a vibration amplitude of  $50 \mu\text{m}$  at  $30 \text{ kHz}$ , a temperature drop of  $60^\circ\text{C}$  is achieved.

The intensity of acoustic streaming induced by longitudinal ultrasonic vibration is found to have strong dependence on the gap between the vibrator and heat source. This phenomenon is not observed with flexural ultrasonic vibration.<sup>2</sup> Analytic analysis proves that resonance of ultrasonic wave significantly increases acoustic streaming velocity. Increase in acoustic streaming velocity is inferred measuring the temperature drop of the heat source. Both experiment and analytic analysis indicate that optimum gaps are the multiple of half-wavelength. Considering the propagation loss of ultrasonic wave, practically applicable optimum gaps correspond to half-wavelength, one full wavelength, and one-and-half wavelength.

Measurements of the temperature distribution in the gap indicate that temperature variations along the radius are insignificant when acoustic streaming is induced, but drastic temperature variations in the direction normal to the vibrating surface occur. The source of acoustic streaming is friction between the physical boundary and high-intensity propagating wave. Inner acoustic streaming velocity induced by friction is used as slip velocity to estimate outer acoustic streaming velocity. As a result, at increasing distance from the heat source the acoustic streaming velocity declines. The threshold distance in which significant convective heat transfer caused by acoustic streaming is observed is found to be 6 mm from the heat source for the gaps of 12 and 24 mm.

The local Nusselt number is calculated to characterize the heat transfer enhancement by acoustic streaming. The dependence of Nusselt number on the local positions ( $r$  and  $z$  direction) in the gap and the separation distance between the walls is analyzed according to the experimental observation. An important optimization design problem is to determine the optimum separation distance between the walls to maximize the convective cooling of the heated plate.

## Acknowledgment

This research was financially supported by Hansung University in 2003.

## References

- Lee, C. P., and Wang, T. G., "Outer Acoustic Streaming," *Journal of the Acoustical Society of America*, Vol. 88, No. 5, 1990, pp. 2367–2375.
- Loh, B., Hyun, S., Ro, P., and Kleinstreuer, C., "Acoustic Streaming Induced by Ultrasonic Flexural Vibrations and Associated Enhancement of Convective Heat Transfer," *Journal of the Acoustical Society of America*, Vol. 111, No. 2, 2002, pp. 875–883.
- Ro, P. I., and Loh, B., "Feasibility of Using Ultrasonic Flexural Waves as a Cooling Mechanism," *IEEE Industrial Electronics*, Vol. 48, No. 1, 2000, pp. 143–150.
- Lighthill, J., "Acoustic Streaming," *Journal of Sound and Vibration*, Vol. 61, No. 3, 1978, pp. 391–418.
- Hamilton, M. F., and Blockstock, D. T., *Nonlinear Acoustics*, Academic Press, New York.

<sup>6</sup>Nyborg, W. L., "Acoustic Streaming near a Boundary," *Journal of the Acoustical Society of America*, Vol. 30, No. 4, 1958, pp. 329–339.

<sup>7</sup>Faraday, M., *Philosophical Transactions of the Royal Society of London*, Vol. 121, 1831, p. 229.

<sup>8</sup>Rayleigh, L., *Theory of Sound*, Dover, New York, 1945.

<sup>9</sup>Schlichting, H., *Boundary Layer Theory*, McGraw-Hill, New York, 1955.

<sup>10</sup>Gopinath, A., and Mills, F., "Convective Heat Transfer From a Sphere due to Acoustic Streaming," *Journal of Heat Transfer*, Vol. 115, April 1993, pp. 332–341.

<sup>11</sup>Gopinath, A., and Mills, F., "Convective Heat Transfer due to Acoustic Streaming Across the Ends of Kundt Tube," *Journal of Heat Transfer*, Vol. 116, Feb. 1994, pp. 47–53.

<sup>12</sup>Vainshtein, P., Fichman, M., and Cutfinger, C., "Acoustic Enhancement of Heat Transfer Between Two Parallel Plates," *International Journal of Heat and Mass Transfer*, Vol. 38, No. 10, 1995, pp. 1893–1899.

<sup>13</sup>Uhlenwinkel, V., Meng, R., Bauckhage, K., Schreckenber, P., and Andersen, O., "Heat Transfer to Cylindrical Bodies and Small Particles in an Ultrasonic Standing-Wave Fields of Melt Atomizer," *Multiphase-Flow and Heat Transfer in Materials Processing*, FED-Vol. 201/HTD-Vol. 297,

American Society of Mechanical Engineers, New York, 1994, pp. 19–24.

<sup>14</sup>Wan, Q., and Kuznetsov, A. V., "Numerical Modeling of Ultrasonic Acoustic Streaming Effect on IC Chips," *Proceedings of 2001 International Mechanical Engineering Congress and Exhibition*, Vol. 1, American Society of Mechanical Engineers, New York, 2001, pp. 1–9.

<sup>15</sup>Wan, Q., and Kuznetsov, A. V., "Effect of Non-Uniformity of Source Vibration Amplitude on the Sound Field Wave Number, Attenuation Coefficient and Reynolds Stress for the Acoustic Streaming," *International Communications in Heat and Mass Transfer*, Vol. 30, No. 1, 2003, pp. 27–36.

<sup>16</sup>Wan, Q., and Kuznetsov, A. V., "Heat Transfer Enhancement by Utilizing Standing and Traveling Waves to Generate Acoustic Streaming in a Rectangular Gap," *Proceedings of the 8th Joint AIAA/ASME Thermophysics and Heat Transfer Conference*, AIAA, Reston, VA, 2002, pp. 1–11.

<sup>17</sup>Sashida, T., *An Introduction to Ultrasonic Motors*, Clarendon Press, Oxford, 1993.

<sup>18</sup>Andres, J. M., and Ingard, U., "Acoustic Streaming at High Reynolds Numbers," *Journal of the Acoustical Society of America*, Vol. 25, No. 5, 1953, pp. 928–937.



## AIRCRAFT ENGINE DESIGN, SECOND EDITION

Jack D. Mattingly—University of Washington • William H. Heiser—U.S. Air Force Academy • David T. Pratt—University of Washington

This text presents a complete and realistic aircraft engine design experience. From the request for proposal for a new aircraft to the final engine layout, the book provides the concepts and procedures required for the entire process. It is a significantly expanded and modernized version of the best selling first edition that emphasizes recent developments impacting engine design such as theta break/throttle ratio, life management, controls, and stealth. The key steps of the process are detailed in ten chapters that encompass aircraft constraint analysis, aircraft mission analysis, engine parametric (design point) analysis, engine performance (off-design) analysis, engine installation drag and sizing, and the design of inlets, fans, compressors, main combustors, turbines, afterburners, and exhaust nozzles.

The AEDsys software that accompanies the text provides comprehensive computational support for every design step. The software has been carefully integrated with the text to enhance both the learning process and productivity, and allows effortless transfer between British Engineering and SI units. The AEDsys software is furnished on CD and runs in the Windows operating system on PC-compatible systems. A user's manual is provided with the software, along with the complete data files used for the Air-to-Air Fighter and Global Range Airlifter design examples of the book.

2002, 692 pp, Hardback  
ISBN: 1-56347-538-3  
List Price: \$89.95  
AIAA Member Price:  
\$69.95

### Contents:

- The Design Process
- Constraint Analysis
- Mission Analysis
- Engine Selection: Parametric Cycle Analysis
- Engine Selection: Performance Cycle Analysis
- Sizing the Engine: Installed Performance
- Engine Component Design: Global and Interface Quantities
- Engine Component Design: Rotating Turbomachinery
- Engine Component Design: Combustion Systems
- Engine Component Design: Inlets and Exhaust Nozzles
- Appendices

American Institute of Aeronautics and Astronautics  
Publications Customer Service, P.O. Box 960, Herndon, VA 20172-0960  
Fax: 703/661-1501 • Phone: 800/682-2422 • E-mail: warehouse@aiaa.org  
Order 24 hours a day at [www.aiaa.org](http://www.aiaa.org)



American Institute of Aeronautics and Astronautics

02-0545